Hindawi
Journal of Spectroscopy
Volume 2019, Article ID 4970376, 15 pages
https://doi.org/10.1155/2019/4970376

Research Article

Frequency Spectrum-Based Optimal Texture Window Size Selection for High Spatial Resolution Remote Sensing Image Analysis

Min Cao,[1] **Dongping Ming**,[1,2] **Lu Xu**,[1] **Ju Fang**,[1] **Lin Liu**,[1] **Xiao Ling**,[1] **and Weizhi Ma**[3]

[1]*School of Information Engineering China University of Geosciences (Beijing), 29 Xueyuan Road, Haidian, Beijing, China*
[2]*Polytechnic Center for Natural Resources Big-Data, MNR of China, Beijing 100036, China*
[3]*Beijing Yanqing Municipal Commission of Housing and Urban-Rural Development, 89 Dongwai Avenue, Yanqing, Beijing, China*

Correspondence should be addressed to Dongping Ming; mingdp@cugb.edu.cn

Received 26 April 2019; Revised 20 August 2019; Accepted 31 August 2019; Published 16 September 2019

Academic Editor: Arnaud Cuisset

Image texture is an important visual cue in image processing and analysis. Texture feature expression is an important task of geo-objects expression by using a high spatial resolution remote sensing image. Texture features based on gray level co-occurrence matrix (GLCM) are widely used in image spatial analysis where the spatial scale is especially of great significance. Based on the Fourier frequency-spectral analysis, this paper proposes an optimal scale selection method for GLCM. Different subset textures are firstly upscaled by GLCM with different window sizes. Then the multiscale texture feature images are converted into the frequency domain by Fourier transform. Consequently, the radial distribution and angular distribution curves changing with different window sizes from spectrum energy can be achieved, by which the texture window size can be selected. In order to verify the validity of this proposed texture scale selection method, this paper uses high-resolution fusion images to classify land cover based on multiscale texture expression. The results show that the proposed method combining frequency-spectral analysis-based texture scale selection can guarantee the quality and accuracy of the classification, which further proves the effectiveness of optimal texture window size selection method bases on frequency spectrum analysis. Other than scale selection in spatial domain, this paper casts a novel idea for texture scale selection in the frequency domain, which is meant for scale processing of remote sensing image.

1. Introduction

High spatial resolution remote sensing images contain rich texture information, and accurate description of texture features can effectively distinguish complex land-cover category [1–3]. Traditional texture feature extraction algorithms can be classified into five categories [4]: structural model, statistic model (GLCM, local variance analysis, and semivariance analysis), filter model (Fourier transformation, wavelet transformation, and Gabor filters), random field (Gaussian–Markov), and fractal model. Most recently, deep-learning method was also applied to extract deep texture features automatically [5, 6]. Of all the above methods, some were employed to measure textural characteristics, such as frequency spectrum analysis; others like GLCM texture feature were directly applied to image classification.

A GLCM is a symmetric matrix with each value representing the probability value of the nearest-neighbor gray tone at a given distance and orientation [7]. It reveals the spatial arrangement of gray levels in an image. The GLCM is generally calculated using moving window for every pixel across the whole image, thereof to provide valuable discriminating spatial structure characteristics and to relate variable patterns of different objects. Orientation and moving window size, together known as scale parameters, were the two most important factors influencing the values of GLCM. In the past few decades, GLCM algorithm has been widely used in image segmentation or classification

[8–15], and the results indicated that outcomes were better when combining GLCM-based texture features with spectral features. However, the GLCM has its own flaws, which mainly embodies in the difficulty and randomness of parameter selection. Many previous studies demonstrated that the scale had a great influence on the validity of the GLCM and the further on the classification accuracy [16–19]. Therefore, many scholars have paid great attention to determine optimal GLCM scale parameters [20–26].

Empirical and enumeration methods were frequently used in the determination of a scale parameter for GLCM texture feature. However, an empirical method is easily influenced by subjective mind, and an enumeration method requires mass of redundant computation when selecting the appropriate scale [24]. In addition, the classical local variance method and geostatistics method [27–32] were proposed to select the optimal scale for geo-objects identification, but they only depend on the local statistical features that lead to the inadequate description of complex texture features [33]. More recently, the multiscale method was introduced into remote sensing image analysis [34–36]. For texture extraction, multiscale analysis can greatly improve the classification accuracy. For example, to improve the performance of texture feature expression and solve the uncertainty problems in land cover classification, Lan and Liu proposed a method to construct GLCM with multiscales inspired by domain knowledge [37]. Huang et al. introduced a reasonable scale texture extraction method, in which a timely changeable cooccurrence window size according to the semivariogram analysis was used [38]. Liu et al. and Chen et al. employed J-M distance statistics to select the optimal scale of CLCM texture [39, 40]. Huang proposed an improved algorithm by using dynamic windows to extract texture features [41]. Liu et al. used posterior probability to optimize multiscale texture window [42]. However, it has been practically found that multiscale texture did not absolutely lead to substantial improvement in accuracy. Choosing a global optimal texture scale is still a key issue for texture feature expression and classification.

High-resolution imagery has abundant meaningful information integrating spectral features with shape and texture, and the periodicity and direction of image texture in the frequency domain can more easily reflect its subtle differences than in the spatial domain [43]. There is a wide range of applications of the Fourier transform-based spectral analysis. Pike and Rozema used four independent aspects of topography which were obtained based on variance spectrum analysis to express numerically for landform classification and other geomorphic problems [44]. Perron et al. quantitatively investigated the existence of characteristic landscape scales by analyzing two-dimensional Fourier power spectra derived from high-resolution topographic maps of two landscapes in California [45]. Moreover, Fourier frequency spectrum analysis has been applied to the study of remote sensing image feature recognition or information extraction. Li et al. selected suitable data for the study of karst peak cluster area by comparing the Fourier frequency spectrum energy of images from SAR and TM data [46]. Wu et al. stressed the feasibility of the object recognition method based on energy in the frequency domain, and this method could identify and extract information from high-resolution imagery based on low-frequency and high-frequency recognition marks with matched Gabor filters after direction and frequency selection [47]. Chen et al. proposed a method to determine the optimal spatial scale for high-resolution imagery based on texture frequency analysis and proved that the variation of texture spectrum energy is helpful to select the optimal scale for geo-objects identification [48]. It can be seen that the Fourier frequency spectrum analysis is an effective method in remote sensing image processing. However, the above method paid attention to the scale effect in remote sensing image classification and did not mention the scale effect in texture feature extraction.

Since a statistical analysis of the Fourier spectrum can reflect the scale effect of texture expression, this paper explores the optimal scale selection method for GLCM texture feature by using the Fourier spectrum analysis. Considering the performance and popularity of GLCM, based on the CLCM texture feature images at different scales, contrast was selected and used to analyze a set of frequency spectrum energy statistical curves to determine the optimal scale parameter for GLCM.

Firstly, four typical objects with different texture features in high-resolution imagery are chosen, and then their CLCM texture features with different moving window sizes are extracted and calculated. Next, GLCM texture feature images are converted into the frequency domain and then the multiscale change trend in spectrum energy distribution curves are analyzed at 18 scales. Finally, according to the change in trend, the optimal scale parameter of GLCM could be selected. In addition, this paper uses the local variance method to select the optimal window size and finally compares the effectiveness of the two methods through experimental verification.

2. Methods

2.1. Texture Frequency Spectrum Energy Acquisition and Spectrum Characteristics Analysis. Set $f(x, y)$ is an image function and its size is $N \times N$. In a two-dimensional space, Fourier transform of an image can be expressed in the formula:

$$F(u, v) = \frac{1}{N} \sum_{x=0}^{N-1} \sum_{y=0}^{N-1} f(x, y) \exp\left[-\frac{2\pi k(ux + vy)}{N}\right], \quad k = 0, 1, 2, \ldots, N-1, \tag{1}$$

where u, v is, respectively, the frequency of sine wave in the x, y direction. $F(u, v)$ is a complex number in general, and its Fourier energy spectrum can be expressed as $|F(u, v)|^2 = F(u, v)F*(u, v)$, where $F*$ is the conjugate complex number of $F(u, v)$ and $|F(u, v)|^2$ is a real number, which reflects global information about the image.

Polar coordinates can be used to measure the Fourier energy spectrum [49]. As shown in Figure 1(a), set $F(r, \theta)$ as

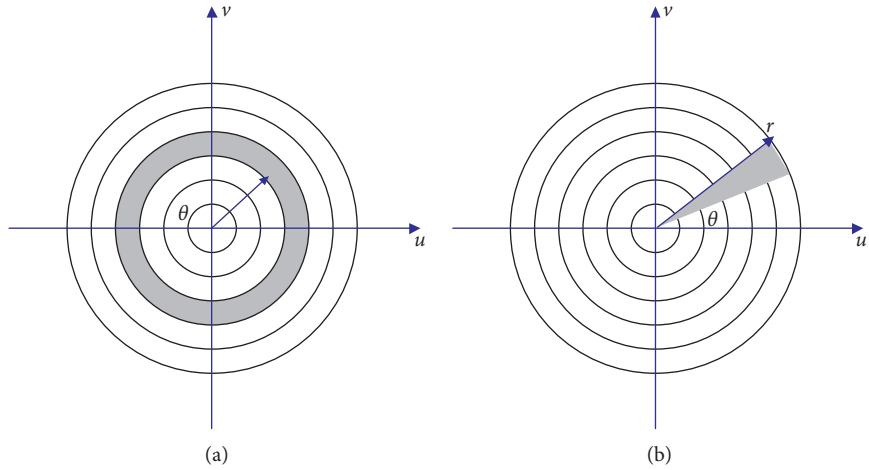

Figure 1: Spectrum energy statistical schematic diagram: (a) radial spectrum energy and (b) angular spectrum energy.

the energy spectrum function, where r and θ are the frequency and direction variables in the polar coordinates, respectively ($r = \sqrt{u^2 + v^2}$ and $\theta = \arctg u/v$). Sum $|F(u,v)|^2$ on a torus centered at the origin by using the formula $F_1(r_1, r_2) = \sum_{r_1^2 \le u^2+v^2 \le r_2^2} |F(u,v)|^2$. Then as shown in Figure 1(b), we can obtain a series of radial spectrum energy statistics, also sum $|F(u,v)|^2$ on a sector from the origin, by using the formula $F_2(\theta_1, \theta_2) = \sum_{\theta_1 \le \arctg u/v \le \theta_2} |F(u,v)|^2$, and then we can obtain a series of angular spectrum energy statistics. Furthermore, setting $\Phi_r = F_1$ and $\Phi_\theta = F_2$ and drawing its curves, we can get a global description of the image frequency spectrum energy. Φ_r represents the radial distribution curve, and Φ_θ represents the angular distribution curve.

Frequency spectrum energy statistics have the following two properties [50]: (1) the peak of the angular spectrum curve corresponds to the main direction of the texture and (2) the position of the peak in the radial spectrum curve corresponds to texture-period in the frequency domain.

To be more specific, Φ_r and Φ_θ can, respectively, describe the thickness and direction distribution of the texture period [51]. Φ_r reflects thickness and periodicity of texture, and here, periodicity means that if the texture unit periodically appears with spatial interval of n pixels, the spectrum energy in the frequency domain is gathered near the ring of which the center is the origin and the radius is $2R/n$ (where R represents the height or width of the image). On the radial distribution curve, the spectrum energy is concentrated at a low frequency when the texture is coarse or at a high frequency when the texture is fine and smooth. Furthermore, peak at a mid and high frequency on the radial distribution curve reflects that texture appears periodically. Φ_θ represents the sensitivity of the spectrum to the texture direction. For instance, if a direction θ on an image contains a lot of lines or edges, the peak of angular spectrum will appear along the $\theta + \pi/2$ direction.

Figure 2 shows four texture subset images with the size of 120×120 pixels, respectively covered with house, farmland, and mixed objects. Figure 2 also shows the spectrum characteristics corresponding to the four texture subset images. Then the spectrum energy can be statistically calculated and shown in Figure 3.

Figure 3 shows the angular and radial spectrums of the four subset textures, from which, it can be explained as follows.

The texture of house is coarse, which determine that spectrum energy is concentrated in low frequency; single house arranged repeatedly leads to more than one peak ($r = 1$, $r = 7$, $r = 12$) in radial distribution curve, which ($r = 7$, $r = 12$) reflects the periodicity of the texture. The angular spectral energy concentrates at 90° and 170° around, which indicates that the house texture represents horizontal and vertical distributions.

As shown in Figure 2(b), the texture feature in Farmland_1 is fine, smooth, and horizontally distributed, while the peak of its angular distribution curve appears near at 90° around and radial spectral energy concentrates at a low frequency ($r = 1$) and a medium frequency ($r = 22$), which indicates the texture is thin and periodic.

In the same way, Farmland_2 is of monotonous texture which is vertically distributed as shown in Figure 2(c), while the angular spectral energy peaks at 180° and the radial spectral energy gets peak at a low frequency ($r = 2$) and a medium frequency ($r = 19$), and the peak at $r = 19$ reflects the periodicity of the texture.

As shown in Figure 2(d), the texture of the mixed objects is rough and disordered, while the angular spectral energy is concentrated in the range of $65° < \theta < 100°$, and the radial spectral energy is mainly concentrated at a low frequency.

2.2. Optimal Texture Window Size Selection Method Based on Frequency Spectrum Analysis. As stated above, scale parameter greatly influences GLCM-based texture feature expression. Generally, if the moving window size is set small, the texture feature image is clear and informative while the edge of geo-object is obscure. As the moving window size increases, the texture feature image becomes coarser with sharpness reduced.

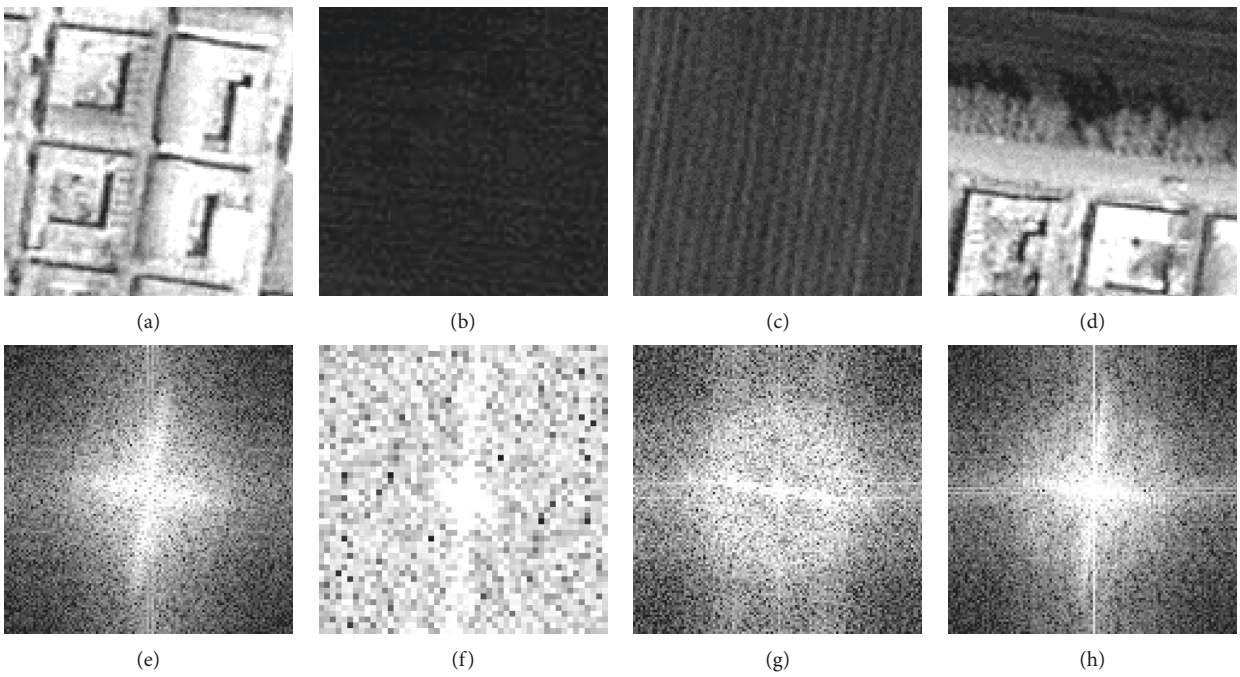

Figure 2: Four subset textures and their spectrum. (a) Houses. (b) Farmland_1. (c) Farmland_2. (d) Image covered with mixed features. (e)–(f) are the related spectrum feature images of (a)–(d).

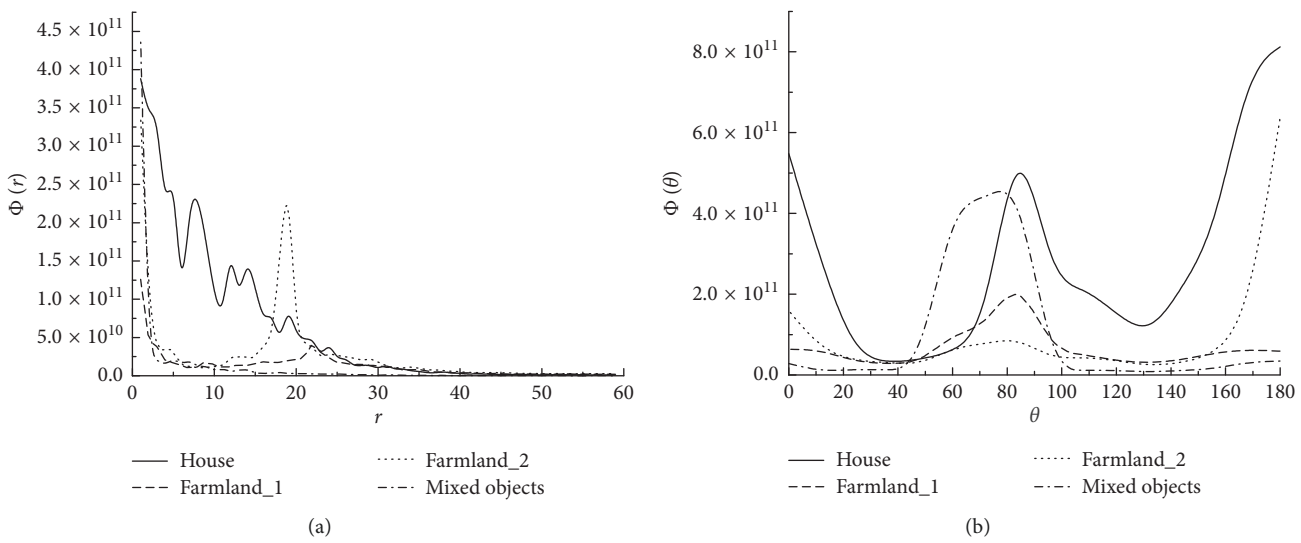

Figure 3: (a) Radial spectrum curve and (b) angular spectrum curve of four different subset textures.

Actually, what changes along with the window size is the direction and period of the texture; that is to say, the orientation and periodicity of the texture feature correspondingly change with the varying window size. As analyzed in Section 2.1, it is clear that the frequency spectrum energy curve of an image can effectively reflect the periodic pattern and direction of texture. Therefore, the frequency spectrum analysis method can be effectively applied to study texture feature images at different scales. Theoretically, if the range of salient regions in a textural image is close to the actual object size at a certain scale, it means the scale can effectively maintain the direction and periodicity of the original texture feature without redundant details; thus, this textural window size can be regarded as the optimal textural analysis scale.

To improve the performance of texture features to distinguish geo-objects categories based on GLCM, this paper combines frequency spectrum knowledge into calculating multiscale texture features based on the Fourier transformation and proposes an optimal textural window size selection method by analyzing the relationship between texture data in spatial and frequency domains. The idea of

this paper is based on theoretical framework of frequency statistics and aims at deducing the spatial geometry features of objects.

Steps for selecting the optimal texture window size are as follows:

(1) Extraction of the multiscale texture images based on GLCM

(2) Plotting the frequency spectrum energy curves of various subset textures on multiscale images

(3) Analysis of radial and angular energy curves of different textures with the change of scale

(4) Selection of the optimal texture scale (or the optimal window size)

3. Experiments

3.1. Experimental Image Data. The experimental image used in this paper is downloaded from Google Maps in the year of 2018. The study area is located in Liujiabao Township, Taiyuan City, Shanxi Province. The size of the study area is 688×737 pixels (Figure 4). The spatial resolution of the experimental image is 0.6 m, and the image data contain three bands (red, green, and blue). The mainland cover types in the study area are house, farmland, road, street trees, bare land, and waterbody, of which house and farmland present clear textural features. As shown in Figure 4 (also as magnified in Figure 2), house, farmland_1, farmland_2, and mixed objects, respectively, marked as (a), (b), (c), and (d), are selected as sample areas for texture frequency spectrum analysis.

Haralick proposed 14 kinds of statistical texture features for GLCM. The eight frequently used statistics are the angular second moment, contrast, correlation, mean, entropy, homogeneity, variance, and dissimilarity. Among them, contrast is the moment of inertia near the principal diagonal line of the GLCM which measures the distribution of matrix values and local variations in image and reflects the clarity of the image and the depth of the texture grooves. After trial and comparison, the contrast feature was chosen for analyzing the optimal texture scale.

The first step of the experiment was to calculate contrast feature with window size ranged from 3×3 to 35×35 and then contrast feature images with different window sizes are shown as Figure 5. Secondly, cutting sample areas are marked as Figures 4(a)–4(d) from the contrast images, and then the Fourier energy spectrum of these four sample areas were converted by the Fourier Transform. Finally energy spectrum was calculated, and we could get a series of radial and angular distribution curves for analysis.

3.2. Analysis of Texture Spectrum Variation at Different Scales. Figures 6(a)–6(d) show the radial and angular distribution curves of four subareas at 18 scales (original image and other 17 upscaling images). With changing of the scale, the variation of their texture spectrum peaks can be analyzed as follows:

(1) As illustrated in Figure 6(a), radial spectrum energy of house texture concentrates in a low-frequency range ($r < 10$) at 18 scales and the positions that the peaks ($r = 7$, $r = 12$) located are consistent, which shows that the change of window size has little effect on house texture period. Angular spectrum energy peaks (Figure 6(a)) at near $\theta = 90^\circ$ and $\theta = 170^\circ$ at 18 scales (due to the horizontal and vertical directions of the house texture), but the peak value varies in different scales. Specifically, the peak energy near $\theta = 90^\circ$ increases from the original image to 3×3 and decreases from 5×5 to 17×17. Similarly, the peak value of 180° increases from the original scale to 9×9 and decreases from 11×11.

(2) As illustrated in Figure 6(b), radial spectrum energy of the original farmland_1 has one main peak and one subpeak, the subpeak indicates that farmland_1 texture is periodic. With the increase of scale, the main peak value disappears and the subpeak value turns left to $r = 15$, and furthermore, both radial and angular spectrum energies reduce greatly starting from 3×3, which is because the textural details are largely neglected with the increase of moving window size.

(3) As shown in Figure 6(c), radial spectrum energy of the original farmland_2 texture concentrates in medium frequency and peak at $r = 19$ and angular curve peak at $\theta = 180^\circ$. However, the textural periodicity and orientation of farmland_2 disappear from 3×3.

(4) As shown in Figure 6(d), with the increase of scale, there is no obvious change on the radial spectrum energy curve. The peak on the angular curve varies differently. From the original scale to 3×3, the peak value firstly reduces and then increases. However, the tendencies of all angular curves maintain consistency with a change of scale.

Further analysis also shows that (1) with the increase of scale, change of the radial curve is sensitive and significant which is represented in decrease in the spectrum energy or the transfer of the peak value; (2) the change of the angular curve is reflected in increase or decrease of peak value; however, tendencies of the curves are relatively steady. (3) When the texture of geo-objects is not obvious, the radial and angular spectrum energies reduce greatly, even disappear with the increase of scale.

3.3. Optimal Texture Window Size Selection Based on Frequency Spectrum. According to the analysis results in Section 3.2, the rules for optimal scale selection for GLCM can be described as follows:

(1) Change of peak value in radial and angular curves can show the variations of frequency spectrum energy with the increase of scale, both of which can be used as the basis of choosing the best scale. Choosing the radial curve for selecting the optimal scale should

Figure 4: Experimental image. (a) House. (b) Farmland_1. (c) Farmland_2. (d) Mixed object.

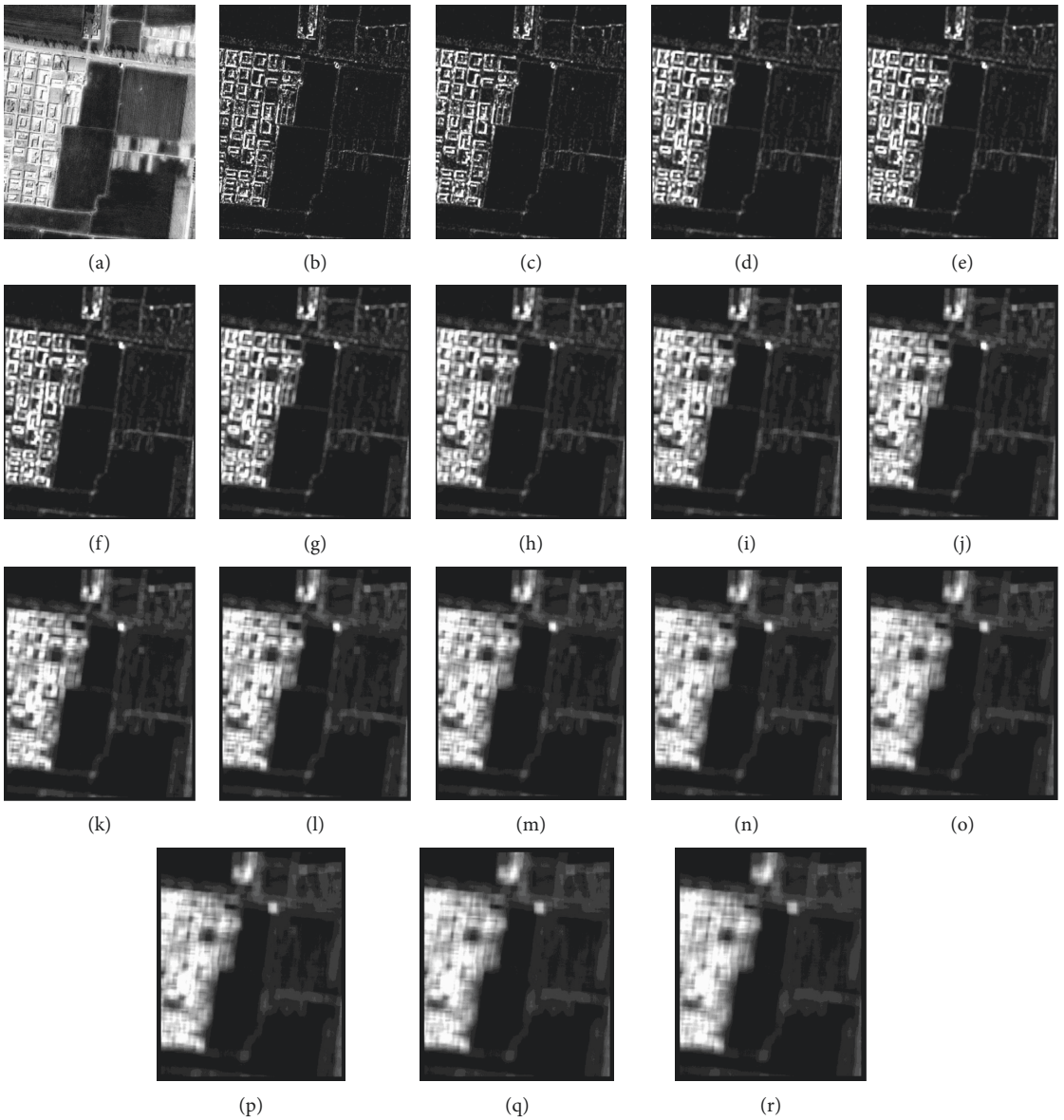

Figure 5: Contrast images at series scale: (a) original image, (b) 3×3, (c) 5×5, (d) 7×7, (e) 9×9, (f) 11×11, (g) 13×13, (h) 15×15, (i) 17×17, (j) 19×19, (k) 21×21, (l) 23×23, (m) 25×25, (n) 27×27, (o) 29×29, (p) 31×31, (q) 33×33, and (r) 35×35.

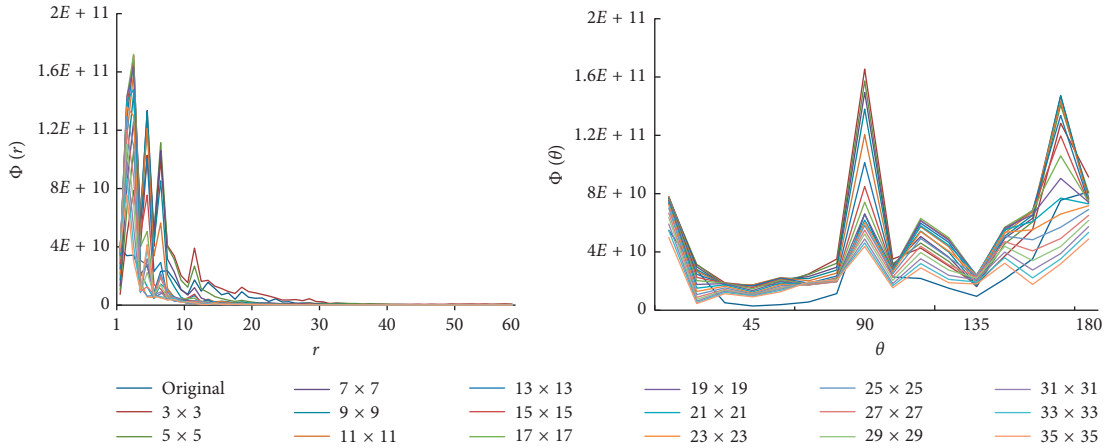

(a)

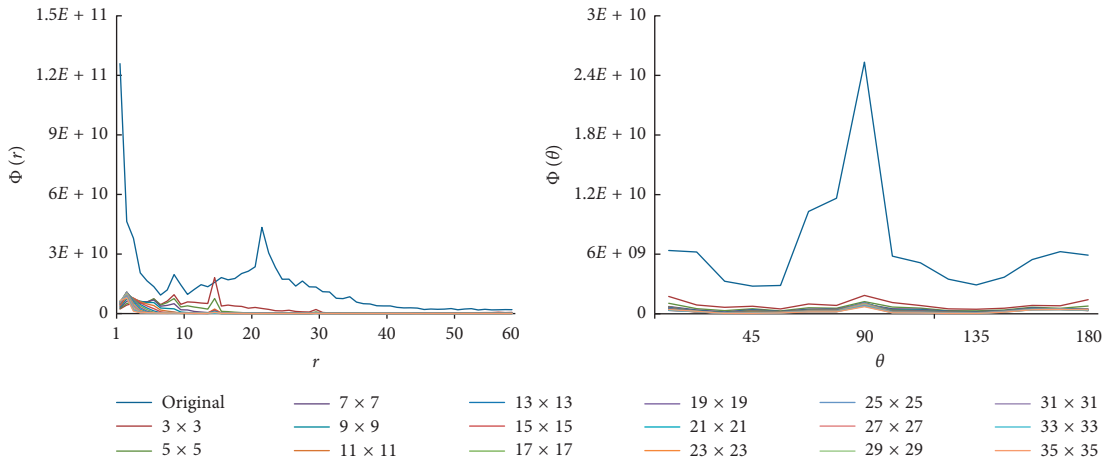

(b)

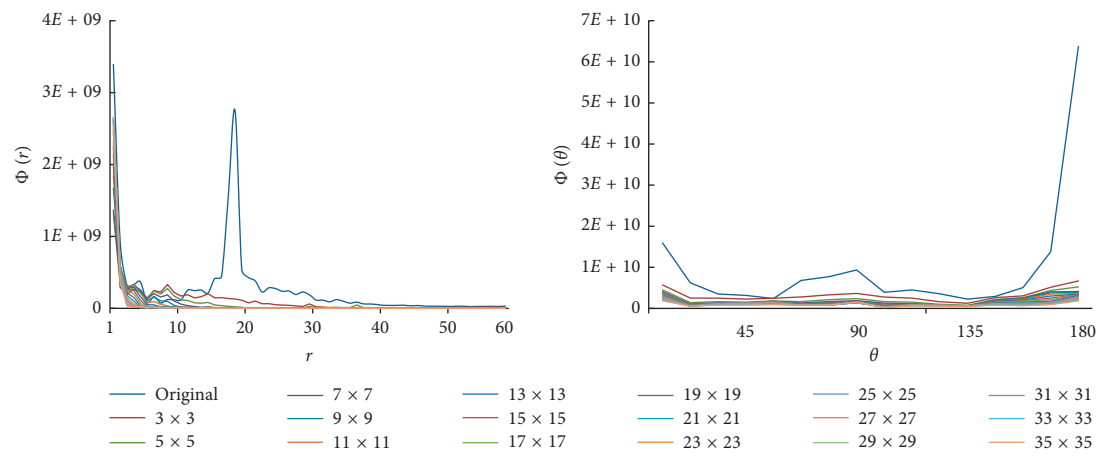

(c)

Figure 6: Continued.

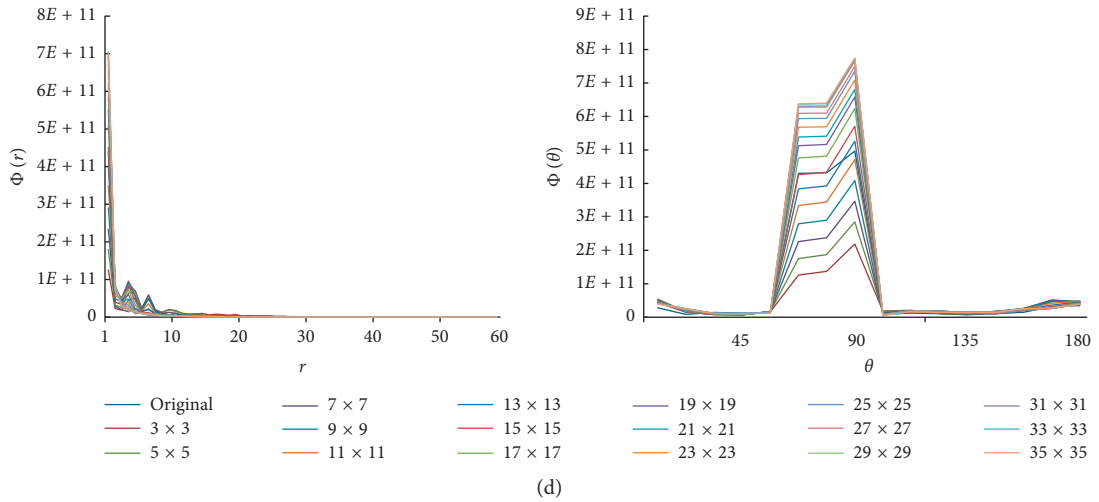

(d)

Figure 6: Radius distribution and angular distribution curves of four subset textures at different scales. Angular and radial spectrum curves of (a) houses, (b) farmland_1, (c) farmland_2, and (d) mixed objects.

take the subpeak as the standard because the subpeak can reflect the period of texture. If there are no double or multiple peaks in the radial curve, the angular spectrum peak can be taken as the criterion.

(2) Compare the frequency spectrum curve on the initial scale with a certain scale, if the peak energy changes dramatically (the peak obviously transfer or shrinks), it indicates that the textural information of original geo-objects cannot be reflected at this scale. However, if the peak value on a scale is consistent with the initial scale, it means that the scale retains the texture information and it can be selected as the optimal texture scale.

(3) For a texture with single and fine characteristics, the larger the window size is, the more texture information is lost, which is because texture feature values calculated by one pixel are closer to its adjacent ones, and they cannot maintain the original neighborhood state of the feature pixel with a large window size. In this case, optimal scale selection can rely on the result of the mixed ground objects.

As shown in Figure 7, the optimal scale of different subset textures in this paper are depicted, respectively, as follows.

For houses, both of the radial and angular spectrum curves can be used as the basis of choosing the best scale. As shown in Figure 7(a), the subpeak value on the radial curve of the original image is located at $r = 7$; in view of the overall trend, the subpeak value increases first and then decreases. The peak at the size 13×13 is consistent with the original image. As shown in Figure 7(b), the peak values on the angular curve are located at $\theta = 90^\circ$ and $\theta = 170^\circ$. With the increase of scale, the peak value shows the same trend as the radial curve. The peak at the size 19×19 is consistent with the original image when $\theta = 90^\circ$. Similarly, for $\theta = 170^\circ$, the energy is consistent with original image on the size of 21×21. Thus, the optimal moving window size was 13×13, 19×19, or 21×21.

For farmland_1 and farmland_2, as shown in Figures 7(c)–7(f), texture frequency spectrum energy greatly reduced, even basically disappeared from scale 2. In this case, the scale can be selected according to the optimal scale of mixed ground objects.

For mixed objects, there is no subpeak on the radial curve, so the changes of the angular curve peak ($\theta = 67^\circ$, $\theta = 90^\circ$) are used to determine the optical scale. Compared with the original scale, the peak value of the frequency spectrum increases first and then decreases. As shown in Figure 7(g), the peak value on the size 15×15 is consistent with the original image when $\theta = 67^\circ$. For $\theta = 90^\circ$, the peak value on the size 13×13 is consistent with the original image. Therefore, the optimal texture window size is 13×13 or 15×15.

According to the analysis presented above, the best classification results can be obtained by using a window size of 13×13, 15×15, 19×19, or 21×21.

3.4. Experimental Verification. Theoretically, the land cover classification result should have higher accuracy with the optimal texture scale selected by the method presented in this paper. To verify the validity of the method, this paper carried out a series of land cover classification experiments based on GLCM features with different moving window sizes from 3×3 pixels to 35×35 pixels. Since SVM (support vector machine) is an effective machine-learning algorithm for high-dimensional data and it could achieve high accuracy even with a small sample amount [52], it is employed to classify the experimental image shown as in Figure 4.

Table 1 shows training sample amounts for each type of geo-object. The training samples were selected by referring Google Maps. For the accuracy evaluation, 1600 test sample points were selected using the stratified sampling method to assess the classification accuracy.

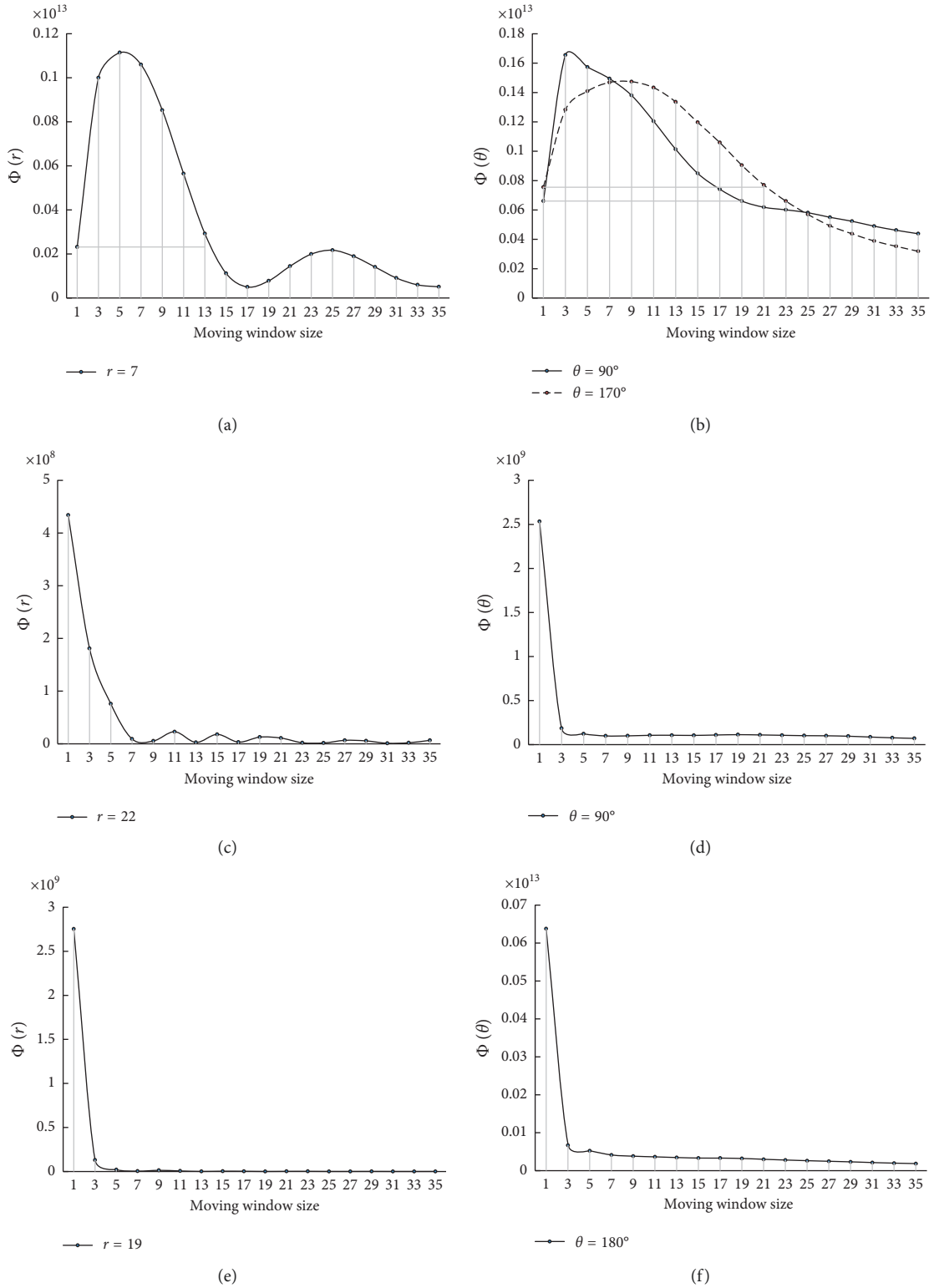

Figure 7: Continued.

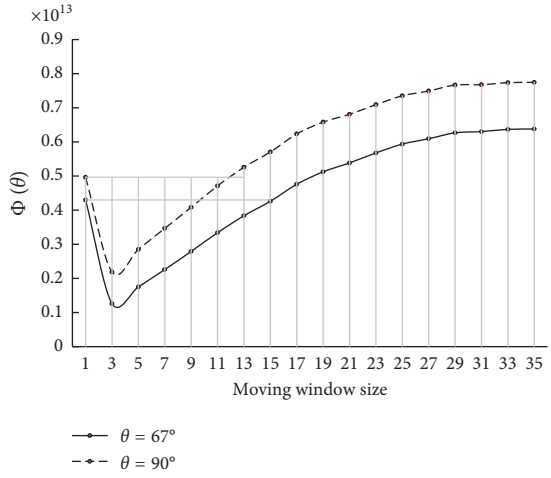

(g)

Figure 7: The peak value change of curves of four subset textures: (a) house radial curve, (b) house angular curve, (c) farmland_1 radial curve, (d) farmland_1 angular curve, (e) farmland_2 radial curve, (f) farmland_2 angular curve, and (g) mixed ground objects angular curve.

Table 1: Number of samples for different geo-objects.

Geo-objects	Training samples	Test samples
Farmland_1	6230	775
Farmland_2	1097	168
House	1284	386
Road	592	63
Bare land	1832	150
Tree	152	28
Waterbody	173	30
Total	11360	1600

Classification experiment consists of 18 groups: the first is to directly classify the original image only based on spectral features; other 17 groups involve texture features into the classification in which the feature vector is composed of 24 features (HOM, CON, DIS, ENT, VAR, ASM, COR, and MEAN of the three original bands) calculated by using different moving window sizes. The classification results are shown in Figure 8.

As can be seen from Figure 8, the classification result based only on spectral features is fragmented, especially it is difficult to distinguish house, bare land, and road objects. Besides, as illustrated in Figure 8(a), there are unclassified pixels for tree and road and misclassification between farmland_1 and farmland_2. Comparing the classification results as shown in Figures 8(b)~8(r), textural details were ignored with increasing moving window size (e.g., house, tree, and bare land), the differences between different objects become larger and the boundaries between them become more distinct.

To assess the accuracies of classification results, this paper employs a confusion matrix [53] to calculate overall accuracies, kappa coefficients (as shown in Figure 9), and producer accuracies of different objects on different scales.

Figure 9 shows that classification accuracy gradually increases with the increase in moving window size. However, when the window size exceeded 17×17, the accuracy decreases slowly. The window size corresponding to the highest accuracy is 15×15, meanwhile the classification accuracy around this window size is better than those of others.

Figure 10 plots the producer accuracies (Prod. Acc.) of different categories in different window sizes. From Figure 10, the following can be observed:

(1) Since the texture of farmland_1 is not obvious, the change of the moving window size has little effect on farmland_1, which results in the accuracy being maintained at a relatively high level.

(2) With the increase in the moving window size, the texture details inside farmland_2 are ignored. The larger the window size used, the lesser the texture detail. Therefore, classification accuracy is mainly determined by spectral features and thus gets higher because crop is sensitive to spectrum. When the window size approaches to 17×17, the accuracy is maintained at a high level.

(3) The Prod. Acc. curves of bare land, road, and tree have the same change tendency (increasing first and then decreasing). It can be deduced that it is effective to improve classification accuracy by setting large moving window size for these kinds of categories. However, it is not true that "the bigger the scale, the higher the accuracy" because when large scale is used, more information will be ignored, which results in misclassification or unclassification.

(4) From the analysis of Section 3.3, the optimal scale of the house based on the radial curve is determined as 13×13, based on the angular curve are 19×19 and 21×21, and the accuracy at the three scales are 90.75, 90.03, and 92.21, respectively (as shown in Figure 10). The experimental result verifies that the house does get a high classification accuracy at the size 21×21.

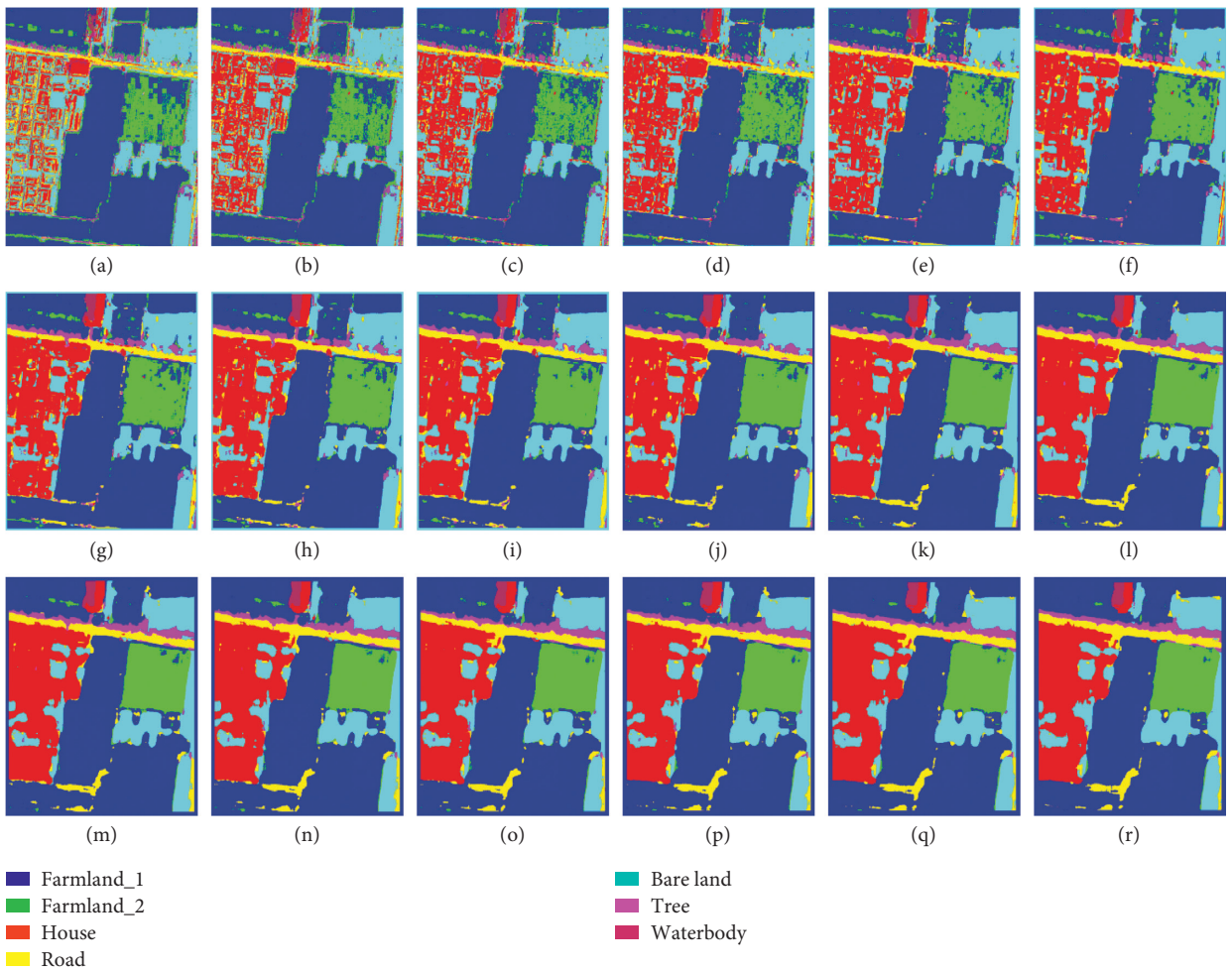

Figure 8: Series of classification results. (a) Only based on spectral features, (b) 3×3, (c) 5×5, (d) 7×7, (e) 9×9, (f) 11×11, (g) 13×13, (h) 15×15, (i) 17×17, (j) 19×19, (k) 21×21, (l) 23×23, (m) 25×25, (n) 27×27, (o) 29×29, (p) 31×31, (q) 33×33, and (r) 35×35.

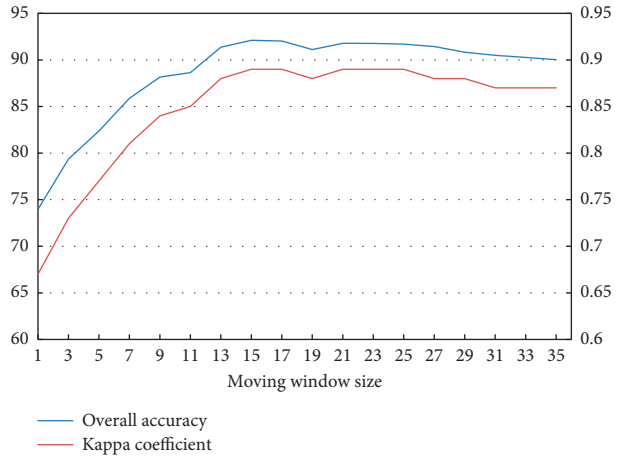

Figure 9: Overall accuracy and kappa coefficient on different scales.

However, the overall accuracy is affected by the six kinds of geo-objects, and high precision of the house does not represent global accuracy. In contrast, the optimal scale of mixed objects are 13×13 and 15×15, and the highest accuracy is achieved on scale 15×15 in experimental result, and the higher accuracies are achieved on scale 13×13 and 17×17.

Generally, these three sizes are consistent with the determined optimal window sizes by using the proposed method. The experimental results show that the optimal scale selection method based on frequency spectrum texture analysis can effectively ensure the classification accuracy.

3.5. Comparisons between Frequency Spectrum Method and Local Variance Method

3.5.1. Optimal Texture Window Size Selection Based on Local Variance. Local variance is a scene texture statistic that has been used to characterize the relationship between spatial scale and object size in the scene. Woodcock and Strahler originally used a 3×3 window and degraded images to coarser levels to examine the change in local variance as pixel size [54] to select the optimal spatial resolution. Similarly, instead of changing pixel sizes, increasing window sizes could be used [55]. By examining a single image, several window sizes and orientations could be used to establish the

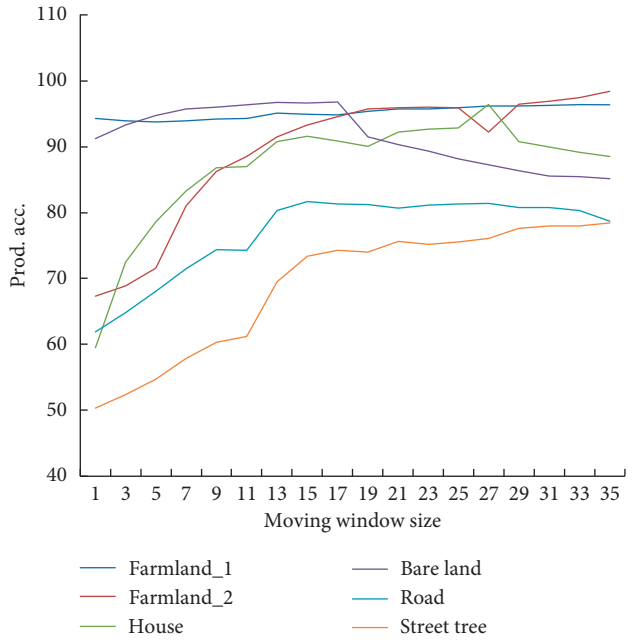

Figure 10: Producer accuracy curves of objects in different scales.

scale and form of autocorrelation based on changes in variance levels [56]. Based on this method, we obtain the local variance curves of four different subset textures, as shown in Figure 11.

Figure 11 shows that it is difficult to use local variance to select the optimal scale because there is no obvious inflection point on local variances. According to the slope of the curves (for more details about the principle of using local variance to select the optimal scale, refer to [54, 57]), it can be determined that the optimal window scale of the house is 17×17, farmland_1 is 7×7, farmland_2 is 9×9, and mixed objects is 13×13.

3.5.2. Comparison and Analysis. Table 2 shows the optimal scale, respectively, selected by the frequency spectrum method and the local variance method, as well as the best scale in the experiment.

Firstly, the frequency spectrum method is more accurate than the local variance method for subset textures with significant texture, such as house and mixed-objects. Secondly, when choosing the global optimal texture scale, the frequency spectrum method performs better than the local variance method. According to the spectrum analysis of house and mixed-objects, it can be quickly determined that the global optimal texture scale is 13, 15, or 17; however, it is somewhat difficult to use the local variance method to determine an appropriate global optimal window size because the optimal scale span of the four objects is relatively large; if the local variance results of the house and mixed objects are used to select the optimal scale, 13 and 17 would be the selected scales, but the two scales did not result the best classification accuracies.

On the other hand, the frequency spectrum method performs better than the local variance in determining the

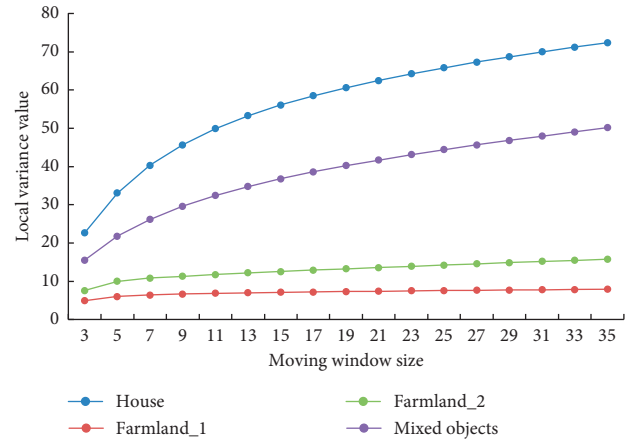

Figure 11: Local variance curve of four different subset textures.

Table 2: Optimal scale selected by different methods.

Subset textures	Frequency spectrum method	Local variance method	Best scale in experiment
House	13×13, 19×19, 21×21	17×17	21×21
Farmland_1	None	7×7	None
Farmland_2	None	9×9	17×17
Mixed-objects	13×13, 15×15	13×13	15×15
Global optimal scale	13×13, 15×15		15×15

optimal scale of different subset textures. Comparing Figure 7 with Figure 11, it can be seen that the spectrum curve of geo-objects has a peak value, and the change of peak value is obvious with the change of scale, so it is easy to find the optimal window size; while the change of local variance curve is relatively flat and there is no obvious inflection point, so it is practically difficult to use the local variance method to determine the optimal scale.

4. Conclusions

Scale selection for textural feature expression is always troublesome in information extraction from remote sensing images. Based on the texture frequency spectrum analysis of four subset textures and peak variation with different window sizes, this paper presents a method based on texture spectrum statistics to determine optimal GLCM scale parameter for high spatial resolution image analysis. According to experimental results, the conclusions are as follows:

(1) It is a feasible way to use the frequency spectrum energy curve of GLCM contrast feature image to effectively reflect the periodic pattern and direction of texture. It casts a novel approach for scale selection of remote sensing image analysis from the frequency domain, which is the main contribution of this work.

(2) The change of the GLCM scale parameter leads to the change of the spectrum energy peak of the subset textures, and the change of peak values can be used as the basis for the optimal scale selection. In practice, the texture of the remote sensing image is complex and aperiodic, but the direction of texture generally exists, so it is easier to obtain the angular peak value than the radial peak value. Therefore, angular peak variation can be preferentially considered in application. The optimal scale of feature extraction needs to be determined by subset textures on remote sensing imagery. In comparison with single subset textures, peak variation on the spectrum curve of mixed objects performs better in determining the global optimal scale.

(3) The combination of texture features based on GLCM can be directly used in a high-resolution remote sensing image classification. Also, the proposed method is the image feature statistics in the frequency domain. Theoretically, it can be used in the selection of segmentation scale parameters. Although how to assess accuracies in object-based image classifications is still an open question, some currently used quantitative segmentation evaluation indexes [58] can be used to evaluate performances of scale quantification.

(4) The scale factor is dependent on the correspondence between spatial scale and object features itself, so it is less realistic to obtain an absolutely optimal scale suitable for all features on the image; however, it is a compromise to get a relatively optimal scale by using the proposed frequency spectrum statistics method.

(5) When the images are mosaics of different classes or features because of the scale dependence of geo-object, stratified scale processing [3, 59] is necessary. As is known, the same kind of objects often have the similar spatial scale and often cluster in a local area, so the image can be roughly divided into some local regions within which the same objects gather and then the proposed texture scale selection method can be used within each local regions. Region partition-based texture scale selection and parallel computing is a viable way to high-performance remote sensing applications.

Data Availability

The high-resolution remote sensing imagery used to support our work were supplied by Arceyes Softwere Maps Downloader under license and so cannot be made freely available. These data are available to access via the website http://m.rivermap.cn/.

Conflicts of Interest

The authors declare no conflicts of interest.

Authors' Contributions

Cao Min conceived, designed, and performed the experiments and wrote the paper. Ming Dongping proposed the research idea and supervised the research and revised the manuscript. Lu Xu, Ju Fang, Lin Liu, and Xiao Ling helped to perform the experiments. Weizhi Ma provided significant comments and suggestions.

Acknowledgments

This research was supported by the National Natural Science Foundation of China (41671369), the National Key Research and Development Program (2017YFB0503600), and "The Fundamental Research Funds for the Central Universities."

References

[1] F. Agüera, F. J. Aguilar, and M. A. Aguilar, "Using texture analysis to improve per-pixel classification of very high resolution images for mapping plastic greenhouses," *ISPRS Journal of Photogrammetry and Remote Sensing*, vol. 63, no. 6, pp. 635–646, 2008.

[2] S. Berberoglu, P. J. Curran, C. D. Lloyd, and P. M. Atkinson, "Texture classification of Mediterranean land cover," *International Journal of Applied Earth Observation and Geoinformation*, vol. 9, no. 3, pp. 322–334, 2007.

[3] W. Zhou, D. P. Ming, L. Xu, H. Bao, and M. Wang, "Stratified object-oriented image classification based on remote sensing image scene division," *Journal of Spectroscopy*, vol. 2018, Article ID 3918954, 11 pages, 2018.

[4] H. Q. Li, Z. K. Liu, and F. Liu, "Aerial image classification method based on fractal theory," *Journal of Remote Sensing*, vol. 5, no. 5, pp. 353–357, 2001.

[5] X. W. Lv, D. P. Ming, T. T. Lu, K. Zhou, M. Wang, and H. Bao, "A new method for region-based majority voting CNNs for very high resolution image classification," *Remote Sensing*, vol. 10, no. 12, Article ID 10121946, 2018.

[6] X. Lv, D. Ming, Y. Chen, and M. Wang, "Very high resolution remote sensing image classification with SEEDS-CNN and scale effect analysis for superpixel CNN classification," *International Journal of Remote Sensing*, vol. 40, no. 2, pp. 506–531, 2019.

[7] R. M. Haralick, K. Shanmugam, and I. H. Dinstein, "Textural features for image classification," *IEEE Transactions on Systems, Man, and Cybernetics*, vol. 3, no. 6, pp. 610–621, 1973.

[8] M. Hanta-Kasari, J. Parkkinen, T. Jaaskelainen, and R. Lenz, "Generalized co-occurrence matrix for multispectral texture analysis," in *Proceedings of 13th International Conference on Pattern Recognition*, vol. 2, pp. 785–789, Vienna, Austria, August 1996.

[9] Z. Lan and Y. Liu, "Study on multi-scale window determination for GLCM texture description in high-resolution remote sensing image geo-analysis supported by GIS and domain knowledge," *ISPRS International Journal of Geo-Information*, vol. 7, no. 5, p. 175, 2018.

[10] Y. F. Hu, L. J. Deng, X. H. Kuang et al., "Study on land use classification of high resolution remote sensing image based on texture feature," *Geography and Geo-Information Science*, vol. 27, no. 5, pp. 692–698, 2011.

[11] M. A. Shaban and O. Dikshit, "Improvement of classification in urban areas by the use of textural features: the case study of

Lucknow city, Uttar Pradesh," *International Journal of Remote Sensing*, vol. 22, no. 4, pp. 565–593, 2001.

[12] F. Pacifici, M. Chini, and W. J. Emery, "A neural network approach using multi-scale textural metrics from very high-resolution panchromatic imagery for urban land-use classification," *Remote Sensing of Environment*, vol. 113, no. 6, pp. 1276–1292, 2009.

[13] Y. Qiu and D. Ming, "Lithostratigraphic classification method combining optimal texture window size selection and test sample purification using Landsat 8 OLI data," *Open Geosciences*, vol. 10, no. 1, pp. 565–581, 2018.

[14] C. S. Hamsa, K. D. Kanniah, F. M. Muharam et al., "Textural measures for estimating oil palm age," *International Journal of Remote Sensing*, vol. 40, no. 19, pp. 7516–7537, 2018.

[15] J. Chen, M. Deng, X. Mei, T. Chen, Q. Shao, and L. Hong, "Optimal segmentation of a high-resolution remote-sensing image guided by area and boundary," *International Journal of Remote Sensing*, vol. 35, no. 19, pp. 6914–6939, 2014.

[16] L. L. Cui, *Integrative Analysis and Evaluation of the Interpretation Feature in Remote Sensing Image*, Institute of Remote Sensing Applications, Chinese Academy of Sciences, Beijing, China, 2005.

[17] Z. Chen, *Research on High Resolution Remote Sensing Image Classification Technology*, Institute of Remote Sensing Applications, Chinese Academy of Sciences, Beijing, China, 2006.

[18] D. J. Marceau, P. J. Howarth, J. M. Dubois, and D. J. Gratton, "Evaluation of the grey-level co-occurrence matrix method for land-cover classification using SPOT imagery," *IEEE Transactions on Geoscience and Remote Sensing*, vol. 28, no. 4, pp. 513–519, 1990.

[19] H. G. Wang and Y. F. Liu, "Study of image texture feature based on gray level co-occurrence matrix," *Bulletin of Surveying and Mapping*, no. 2, pp. 28–30, 2013.

[20] J. B. K. Kiema, "Texture analysis and data fusion in the extraction of topographic objects from satellite imagery," *International Journal of Remote Sensing*, vol. 23, no. 4, pp. 767–776, 2002.

[21] D. Chen, D. A. Stow, and P. Gong, "Examining the effect of spatial resolution and texture window size on classification accuracy: an urban environment case," *International Journal of Remote Sensing*, vol. 25, no. 11, pp. 2177–2192, 2004.

[22] A. Puissant, J. Hirsch, and C. Weber, "The utility of texture analysis to improve per-pixel classification for high to very high spatial resolution imagery," *International Journal of Remote Sensing*, vol. 26, no. 4, pp. 733–745, 2005.

[23] M. Pesaresi, "Texture analysis for urban pattern recognition using fine-resolution panchromatic satellite imagery," *Geographical and Environmental Modelling*, vol. 4, no. 1, pp. 43–63, 2000.

[24] S. E. Franklin, M. A. Wulder, and M. B. Lavigne, "Automated derivation of geographic window sizes for use in remote sensing digital image texture analysis," *Computers & Geosciences*, vol. 22, no. 6, pp. 665–673, 1996.

[25] G. Zhou and N. S.-N. Lam, "Reducing edge effects in the classification of high resolution imagery," *Photogrammetric Engineering & Remote Sensing*, vol. 74, no. 4, pp. 431–441, 2008.

[26] J. Zhou, R. Y. Guo, M. Sun et al., "The Effects of GLCM parameters on LAI estimation using texture values from Quickbird satellite imagery," *Scientific Reports*, vol. 7, no. 1, p. 7366, 2017.

[27] H. C. Ma and D. R. Li, "Geographic window fixing and its application based on spatial statistics," *Geomatics and Information Science of Wuhan University*, vol. 26, no. 1, pp. 18–23, 2001.

[28] M. Chica-Olmo and F. Abarca-Hernández, "Computing geostatistical image texture for remotely sensed data classification," *Computers & Geosciences*, vol. 26, no. 4, pp. 373–383, 2000.

[29] D. Ming, J. Li, J. Wang, and M. Zhang, "Scale parameter selection by spatial statistics for GeOBIA: using mean-shift based multi-scale segmentation as an example," *ISPRS Journal of Photogrammetry and Remote Sensing*, vol. 106, no. 8, pp. 28–41, 2015.

[30] D. Ming, J. Du, X. Zhang, and T. Liu, "MALV for pixel-level scale selection of multi-band remote sensing images and its scale effect on image classification accuracy," *Journal of Applied Remote Sensing*, vol. 7, no. 18, p. 3565, 2013.

[31] D. Ming, T. Ci, H. Cai, L. Li, C. Qiao, and J. Du, "Semivariogram based spatial bandwidth selection for remote sensing image segmentation with mean-shift algorithm," *IEEE Geoscience and Remote Sensing Letters*, vol. 9, no. 5, pp. 813–817, 2012.

[32] A. Yue, C. Zhang, J. Yang, W. Su, W. Yun, and D. Zhu, "Texture extraction for object-oriented classification of high spatial resolution remotely sensed images using a semivariogram," *International Journal of Remote Sensing*, vol. 34, no. 11, pp. 3736–3759, 2013.

[33] M. F. Goodchild, "Metrics of scale in remote sensing and GIS," *International Journal of Applied Earth Observation and Geoinformation*, vol. 3, no. 2, pp. 114–120, 2001.

[34] J. Chen, T. Q. Chen, X. M. Mei, Q. Shao, and M. Deng, "Hilly farmland extraction from high resolution remote sensing imagery based on optimal scale selection," *Transactions of the Chinese Society of Agricultural Engineering*, vol. 30, no. 5, pp. 99–107, 2014.

[35] J. Chen, M. Deng, P. F. Xiao, M. Yang, X. Mei, and H. Liu, "Object-oriented classification of high resolution imagery combining support vector machine with granular computing," *Acta Geodaetica et Cartographica Sinica*, vol. 40, no. 2, pp. 135–147, 2011.

[36] J. Chen, M. Deng, X. M. Mei et al., "Optimal segmentation of high-resolution remote sensing images guided by area and boundary," *International Journal of Remote Sensing*, vol. 35, no. 19, pp. 6914–6939, 2014.

[37] Z. Y. Lan and Y. Liu, "Classification of land-use based on remote sensing image texture features with multi-scales and cardinal direction inspired by domain knowledge," *Acta Geodaetica et Cartographica Sinica*, vol. 45, no. 8, pp. 973–982, 2016.

[38] Y. Huang, C. Zhang, W. Su et al., "A study of optimal scale texture analysis for remote sensing image classification," *Remote Sensing for Land & Resources*, vol. 20, no. 4, pp. 14–17, 2008.

[39] Y. S. Liu, C. W. Lu, F. X. Zhu, and C. Gao, "Extraction of high spatial resolution remote sensing image classification based on PCA and multi-scale texture feature," *Remote Sensing Technology and Application*, vol. 27, no. 5, pp. 706–711, 2012.

[40] L. Chen, Y. J. Zhang, and B. Chen, "High spatial remote sensing image classification based on decision tree classification combined with multiscale texture," *Geography and Geo-Information Science*, vol. 23, no. 4, pp. 18–21, 2007.

[41] X. Huang and W. N. Yang, "Classification of remotely sensed imagery according to the combination of gray scale and texture features based on the dynamic windows," *Journal of Geomatics Science and Technology*, vol. 32, no. 3, pp. 277–281, 2015.

[42] J. X. Liu, H. P. Liu, J. Heiskanen, M. Mõttus, and P. Pellikka, "Posterior probability-based optimization of texture window size for image classification," *Remote Sensing Letters*, vol. 5, no. 8, pp. 753–762, 2014.

[43] G. P. Wu, P. F. Xiao, X. Z. Feng, and K. Wang, "Object recognition for high-resolution remotely sensed imagery based on energy in frequency domain," *Geomatics and Information Science of Wuhan University*, vol. 36, no. 11, pp. 1294–1297, 2011.

[44] R. J. Pike and W. J. Rozema, "Spectral analysis of landforms," *Annals of the Association of American Geographers*, vol. 65, no. 4, pp. 499–516, 2015.

[45] J. T. Perron, J. W. Kirchner, and W. E. Dietrich, "Spectral signatures of characteristic spatial scales and nonfractal structure in landscapes," *Journal of Geophysical Research Atmospheres*, vol. 113, no. F4, article F04003, 2008.

[46] M. Li, H. Wu, M. Hao, Z. Guan, and Y. Liu, "Comparison analysis on texture characteristics of SAR and TM images of the Karst Peak cluster landforms," *Remote Sensing Information*, vol. 28, no. 6, pp. 19–25, 2013.

[47] G. P. Wu, P. F. Xiao, X. Z. Feng et al., "Applying frequency spectrum energy analysis theory and method to recognize objects for renote sensing image," *Geomatics and Information Science of Wuhan University*, vol. 38, no. 12, pp. 1465–1469, 2013.

[48] J. Chen, M. Deng, P. F. Xiao, M. H. Yang et al., "Optimal spatial scale choosing for high resolution imagery based on texture frequency analysis," *Journal of Remote Sensing*, vol. 15, no. 3, pp. 492–511, 2011.

[49] R. C. Gonzalez, R. E. Woods, and E. D. L. Stevenl, *Digital Image Processing Using MATLAB*, Publishing House of Electronics Industry, Beijing, China, 2013.

[50] R. Bamberger and M. J. T. Smith, "A filter bank for the directional decomposition of images: theory and design," *IEEE TransSignal Process*, vol. 40, no. 4, pp. 882–893, 1992.

[51] Y. J. Zhang, *Image Analysis: Second Edition Beijing*, Tsinghua University Press, House of Electronics Industry, Beijing, China, 2005.

[52] C. Huang, L. S. Davis, and J. R. G. Townshend, "An assessment of support vector machines for land cover classification," *International Journal of Remote Sensing*, vol. 23, no. 4, pp. 725–749, 2002.

[53] G. M. Foody, "Status of land cover classification accuracy assessment," *Remote Sensing of Environment*, vol. 80, no. 1, pp. 185–201, 2002.

[54] C. E. Woodcock and A. H. Strahler, "The factor of scale in remote sensing," *Remote Sensing of Environment*, vol. 21, no. 3, pp. 311–332, 1987.

[55] D. M. Chen, "Multiresolution models on image analysis and classification," in *Proceedings of the UCGIS Summer Assembly and Retreat*, Bar Harbor, ME, USA, February 1998.

[56] D. Ming, J. Yang, L. Li, and Z. Song, "Modified ALV for selecting the optimal spatial resolution and its scale effect on image classification accuracy," *Mathematical and Computer Modelling*, vol. 54, no. 3-4, pp. 1061–1068, 2011.

[57] Y. N. Ma, D. P. Ming, and H. P. Yang, "Scale estimation of object-oriented image analysis based on spectral-spatial statistics," *Journal of Remote Sensing*, vol. 21, no. 4, pp. 566–578, 2017.

[58] Y. Chen, D. Ming, L. Zhao, B. Lv, K. Zhou, and Y. Qing, "Review on high spatial resolution remote sensing image segmentation evaluation," *Photogrammetric Engineering & Remote Sensing*, vol. 80, no. 10, pp. 629–646, 2018.

[59] X. Lu, D. Ming, W. Zhou, H. Bao, Y. Chen, and X. Ling, "Farmland extraction from high spatial resolution remote sensing images based on stratified scale pre-estimation," *Remote Sensing*, vol. 11, no. 2, p. 108, 2019.